Pergamon

Neuropharmacology 43 (2002) 595–606

NEURO PHARMACOLOGY

www.elsevier.com/locate/neuropharm

Chronic benzodiazepine administration alters hippocampal CA1 neuron excitability: NMDA receptor function and expression[1]

B.J. Van Sickle [a], A.S. Cox [a], K. Schak [a], L. John Greenfield Jr. [a,b], E.I. Tietz [a,*]

[a] *Department of Pharmacology, Medical College of Ohio, Block Health Science Building, 3035 Arlington Ave, Toledo, OH 43614, USA*
[b] *Department of Neurology, Medical College of Ohio, Toledo, OH 43614, USA*

Received 10 May 2002; received in revised form 28 June 2002; accepted 16 July 2002

Abstract

Rats are tolerant to benzodiazepine (BZ) anticonvulsant actions two days after ending one-week administration of the BZ, flurazepam (FZP). Concurrently, $GABA_A$ receptor-mediated inhibition is reduced and AMPA receptor-mediated excitation is selectively enhanced in CA1 pyramidal neurons in hippocampal slices. In the present study, the effects of chronic FZP exposure on NMDA receptor (NMDAR) currents were examined in CA1 pyramidal neurons in hippocampal slices and following acute dissociation. In CA1 neurons from chronic FZP-treated rats, evoked NMDAR EPSC amplitude was significantly decreased (52%) in slices, and the maximal current amplitude of NMDA-induced currents in dissociated neurons was also significantly reduced (58%). Evoked NMDAR EPSCs were not altered following acute desalkyl-FZP treatment. Using in situ hybridization and immunohistochemical techniques, a selective reduction in NR2B subunit mRNA and protein expression was detected in the CA1 and CA2 regions following FZP treatment. However, total hippocampal NMDAR number, as assessed by autoradiography with the NMDAR antagonist, [^{3}H]MK-801, was unchanged by FZP treatment. These findings suggest that reduced NMDAR-mediated currents associated with chronic BZ treatment may be related to reduced NR2B subunit-containing NMDARs in the CA1 and CA2 regions. Altered NMDAR function and expression after chronic BZ exposure may contribute to BZ anticonvulsant tolerance or dependence.

Keywords: NMDA receptor; Tolerance; Flurazepam; EPSCs; CAI; Excitatory synapses

1. Introduction

Benzodiazepines (BZs) are positive allosteric modulators of γ-aminobutyric acid type A receptors (GABARs). BZs increase GABA affinity and thereby increase the frequency of Cl^- channel opening, potentiating GABAR-mediated inhibitory responses in the central nervous system (Macdonald and Olsen, 1994). The ability of BZs to modulate CNS inhibition makes them an attractive clinical therapy in treating disorders of altered neuronal excitability such as epilepsy, sleep disturbances, and generalized anxiety. However, the clinical usefulness of BZs, especially as anticonvulsants, is limited by development of tolerance which occurs with the prolonged administration required to treat these chronic disorders. BZ tolerance has been extensively studied in GABAergic inhibitory systems, particularly in the hippocampus since it is often a locus for epileptic activity. Accordingly, changes in GABAR structure, function and pharmacology, thought responsible for BZ tolerance, have been well described (Hutchinson et al., 1996).

Rats chronically treated with the BZ, flurazepam (FZP), demonstrate BZ tolerance in vivo (Rosenberg, 1995) and in vitro (Xie and Tietz, 1992; Zeng and Tietz, 1999), but more interestingly, CA1 pyramidal neurons from chronic FZP-treated rats demonstrate significant changes in synaptic function. GABAergic inhibition is reduced in CA1 pyramidal neurons but not dentate granule (DG) neurons (Zeng et al., 1995; Poisbeau et al., 1997; Zeng and Tietz, 1999), while α-amino-3-hydroxy-5-methyl-4-isoxazolepropionic acid receptor (AMPAR)-mediated excitation is increased in CA1 pyramidal neurons, but not DG neurons (Van Sickle and Tietz, 2000b).

* Corresponding author. Tel.: +1-419-383-4182; fax: +1-419-383-2871.
E-mail address: etietz@mco.edu (E.I. Tietz).

[1] Portions of this manuscript have been published in abstract form: Society for Neuroscience Abstracts 25:391.5, 1999 and 27:262.3, 2001.

0028-3908/02/$ - see front matter © 2002 Elsevier Science Ltd. All rights reserved.
PII: S0028-3908(02)00152-1

Moreover, GABAR-mediated depolarizations are observed in CA1 pyramidal neurons following chronic FZP-treatment (Zeng et al., 1995). Since GABAR depolarizations can directly potentiate NMDA-evoked responses in CA1 pyramidal neurons (Staley et al., 1995), these findings suggest altered excitation/inhibition within the CA1 region after chronic FZP-treatment that would be predicted to facilitate NMDAR-mediated excitation in CA1 pyramidal neurons. Subsequent regulation of NMDAR function and subunit expression following modulation of NMDAR-mediated activity may contribute to expression of BZ tolerance or alternatively, dependence.

This study addresses changes in NMDAR function and expression in CA1 pyramidal neurons following chronic BZ treatment. Experiments assessed the effect of 1-week FZP treatment, previously shown to alter GABAR-mediated inhibition and AMPAR-mediated excitation, on the function and expression of NMDARs. Stimulus-evoked excitatory postsynaptic currents (EPSCs) were recorded from CA1 pyramidal neurons using whole-cell patch techniques in in vitro hippocampal slices. In addition, NMDA-induced currents were recorded in acutely dissociated CA1 pyramidal neurons to assess the responsiveness of postsynaptic NMDA receptors. Since regulation of individual GABAR subunit mRNA and protein was correlated with decreased GABAR function in CA1 pyramidal neurons (Chen et al., 1999), alterations in NMDAR subunit mRNA and protein, which may relate to changes in NMDAR function, were analyzed using quantitative in situ hybridization, immunohistochemistry, and receptor autoradiography.

2. Materials and methods

2.1. Drugs and reagents

APV (DL-2-amino-5 phosphonovaleric acid), DNQX (6,7-dinitroquinoxaline-2,3-done), lidocaine *N*-ethyl bromide quaternary salt (QX-314), MK-801, picrotoxin and FZP dihydrochloride were obtained from Research Biochemicals International division of Sigma-Aldrich Chemical Co. (St Louis, MO). The NMDAR channel blocker [^{3}H]MK-801 was from NEN Life Sciences Products, Inc. (Boston, MA). Desalkyl-FZP was from Hoffman-LaRoche Inc. (Nutley, NJ). The $GABA_B$ antagonist, CGP-35348 was a gift from Dr M.F. Pozza (CIBA Geigy AG, Basel, Switzerland). Oligoprobes were purchased from Oligos Etc. Inc. (Willsonville, OR). Antibodies were purchased from commercial sources: polyclonal NR1 and NR2B (Chemicon International, Temecula, CA); biotinylated anti-rabbit IgG $F(ab')_2$ fragments (Boehringer Mannheim, Indianapolis, IN). All other chemicals were from Sigma-Aldrich.

2.2. Benzodiazepine treatment

Experimental protocols involving the use of vertebrate animals were approved by the Medical College of Ohio, Institutional Animal Care and Use Committee (IACUC) and conformed to National Institutes of Health guidelines. One-week FZP treatment was carried out as previously established (Xie and Tietz, 1992; Van Sickle and Tietz, 2002a). Following 2-day adaptation to 0.02% saccharin vehicle, male Sprague–Dawley rats (initial age: P22–25; Harlan, Indianapolis, IN) were offered FZP in 0.02% saccharin water for 1 week (100 mg/kg for 3 days, 150 mg/kg for 4 days) as their sole source of drinking water. Daily water consumption was monitored for each rat and used to adjust drug concentration so that the criterion dose ($>$100 mg/kg/week) of FZP was achieved. Using this protocol, rats are tolerant to BZ suppression of pentylenetetrazole-induced seizures (Rosenberg, 1995). Matched control rats received only saccharin water. At the end of drug administration, rats were offered saccharin water for 2 days before they were euthanized for hippocampal slice preparation, CA1 neuron dissociation or cryostat tissue sectioning. Two days after the end of FZP exposure, residual BZ and metabolites are no longer detectable in hippocampus by radioreceptor assay ($<$3 ng FZP and metabolites/g hippocampus; Xie and Tietz, 1992). To determine whether the hippocampal changes measured were specific to chronic BZ treatment, 2.5 mg/kg of the FZP active metabolite, desalkyl-FZP, was given acutely to another group of rats by gavage 2 days before sacrifice. Food was removed 12 h prior to gavage. Control rats received an equivalent volume of emulsion vehicle [peanut oil, water and acacia (4:2:1)]. The single dose of desalkyl-FZP was previously demonstrated to result in levels of BZ activity similar to that found in the hippocampus of rats after 1-week FZP treatment without a concomitant effect on GABAR-mediated inhibition (Xie and Tietz, 1992) or AMPAR-mediated excitation (Van Sickle and Tietz, 2002a).

2.3. Electrophysiology

2.3.1. Hippocampal slices

Hippocampal slices (450 μm) were prepared from FZP-treated and control rats as described previously (Zeng et al., 1995; Zeng and Tietz, 1999). Briefly, transverse hippocampal slices were prepared on a vibratome (Ted Pella, Inc., Redding, CA) in ice-cold, pregassed (95% O_2/5% CO_2) ACSF containing (in mM): NaCl, 119; KCl, 2.5; $CaCl_2$, 1.8; $MgSO_4$, 1.3; NaH_2PO_4, 1.25; $NaHCO_3$, 26; D-glucose, 10; pH 7.4. Area CA3 was removed during slice preparation to prevent recurrent activation and epileptiform discharges during electrical stimulation in the presence of GABAR antagonists. Slices were maintained at room temperature for $\geq$1 h in

gassed ACSF. During recording, slices were perfused at 2.5 ml/min with gassed ACSF at room temperature.

2.3.2. CA1 neuron dissociation

CA1 pyramidal neurons were acutely isolated using the following modifications of methods described previously (Tietz et al., 1999b). Coronal brain sections (350 μm) were incubated 5 min in 1 mg/ml papain at 37 °C (Kew et al., 1998; F. Knoflach, personal communication) in oxygenated (95% O_2/5% CO_2) PIPES (1,4-piperazinebis(ethanesulfonic acid) buffer (in mM): NaCl, 120; KCl, 2.5; $MgCl_2$, 1; $CaCl_2$, 1.5; D-glucose, 25; PIPES, 20; pH 7.0. Slices were washed 4× for 10 min in PIPES buffer with or without 1 mg/ml bovine serum albumin (BSA). Inclusion of BSA increased the numbers of recordable cells without significantly changing the EC_{50} or maximal current (data not shown; J. Margiotta, personal communication). The hippocampal CA1 region was dissected on ice and three 1 mm fragments of the CA1 region were triturated using a 25 gauge bore Pasteur pipette in 100 μl of ice cold PIPES. Fifty microliters of the cell suspension was plated on each of two poly-lysine-coated (2 mg/ml, poly-D-lysine; 2 mg/ml, poly-DL-lysine) culture dishes for 15–45 min prior to recording.

2.3.3. Electrophysiological recording

NMDAR-mediated, stimulus-evoked EPSCs were recorded from CA1 pyramidal neurons in in vitro hippocampal slices by stimulation of the Schaffer collateral pathway in the presence of 10 μM DNQX, 10 μM glycine, 25 μM CGP-35348 and 50 μM picrotoxin using whole-cell voltage-clamp techniques as described previously (Zeng and Tietz, 1999). Briefly, patch pipettes (5–9 MΩ) were filled with internal solution containing (in mM): Cs-methanesulfonate, 132.5; CsCl, 17.5; HEPES, 10; EGTA, 0.2; NaCl, 8; Mg-ATP, 2; Na_3-GTP, 0.3; QX-314, 2; pH 7.2 adjusted with CsOH. Cs^+ was included to block $GABA_B$-mediated K^+ currents. Neurons were voltage-clamped from −80 to +40 mV in continuous mode (cSEVC) using an Axoclamp 2A amplifier (Axon Instruments Inc., Union City, CA). Cells in which the holding current changed by more than 20% or the seal degraded were abandoned. NMDAR-mediated EPSCs were elicited with a tungsten, bi-polar stimulating electrode at a stimulus intensity (~0.1–0.8 mAmps) half-maximal for the EPSC. Current output was low-pass filtered (10 kHz), DC-offset and amplified 10,000-fold. The signal was continuously monitored on-line (PClamp 6.0 Software, Axon Instruments) and digitized (Digidata 1200, Axon) at a sampling frequency of 10 kHz. Current–voltage (*I–V*) curves were compared by repeated measures ANOVA followed by post hoc analysis by the method of Scheffé.

Whole-cell voltage clamp ($V_h = -30$mV) recordings in acutely dissociated CA1 pyramidal neurons were made at room temperature (22–24 °C) in extracellular recording solution containing (in mM): NaCl, 140; KCl, 2.5; $CaCl_2$, 2.0; D-glucose, 10; and HEPES, 10; pH 7.4, 320–325 mOsm. The patch-pipette internal solution contained (in mM): $CsCH_3SO_3$, 150; NaCl, 5; HEPES, 10; EGTA, 0.2; and an ATP regeneration system [CPK, 50 U/ml; phosphocreatine, 25; Na-ATP, 2; Mg-ATP, 2; and Na_3-GTP, 0.3; pH 7.3, 305–310 mOsm]. Patch-pipettes were glass capillaries pulled to a tip resistance of 3–7 MΩ (1.5 mm OD micro-hematocrit glass, Fisher Scientific, Pittsburgh, PA, USA). To facilitate gigaohm seal-formation, pipettes tips were filled with internal solution minus the ATP regeneration system (290–295 mOsm), then back-filled with internal solution. Whole-cell currents were recorded with an Axoclamp 200-B amplifier (Axon), displayed on a Gould TA-240 thermal chart recorder and recorded for later analysis onto computer hard disk using a Digidata 1200B AD/DA converter and PCLAMP 8.0 acquisition software (Axon). Series resistance and cell capacitance were compensated prior to the experiment and monitored throughout. For concentration–response studies, cells were visualized (40×) on an upright microscope (Nikon TE200, Dexter, MI) using Hoffman DIC optics. Only cells with distinct pyramidal shape and of similar size were selected.

Drugs were applied to dissociated CA1 neurons using a gravity-driven, modified U-tube 'multipuffer' drug application system (Greenfield and Macdonald, 1996; Tietz et al., 1999b). Solutions were dissolved in extracellular buffer to the desired concentrations from the following stock solutions: 10 mM glycine and 10 mM GABA in H_20, 10 mM strychnine and 100 mM NMDA in DMSO (dimethylsulfoxide). Drugs dissolved in DMSO were further diluted in extracellular buffer to a final concentration of <0.05%, previously determined to have no effect on GABAR whole-cell currents (Tietz et al., 1999b). Co-applied drug solutions were maintained in the same drug reservoir. NMDA concentration–response relationships were evaluated by measuring the maximal current elicited by a 10 s application of increasing concentrations (1–3000 μM) of NMDA, co-applied with 10 μM glycine and 20 μM strychnine at 2 min intervals.

Peak NMDAR current amplitudes were analyzed at each concentration for individual cells. NMDA concentration–response data for individual cells and for the pooled cells from control and 1-week FZP-treated rats were fit to a one-site model using PRISM software (GRAPHPAD, San Diego, CA) with the equation: $I = (I_{min} + I_{max}([NMDA]^n/EC_{50}^n)) / (1 + [NMDA]^n / EC_{50}^n)$ where I was the current at a given NMDA concentration. I_{min} the current in the absence of NMDA and I_{max} was the current evoked by a saturating NMDA concentration. The Hill slope (n_H) was allowed to vary. The EC_{50} was derived from the best-fit equation. Statistical differences were

calculated based upon fits of concentration–response data from individual cells.

2.4. mRNA and protein expression and receptor autoradiography

2.4.1. Brain section preparation

Two-days following 1-week FZP treatment, control and FZP-treated rats were deeply anesthetized with sodium pentobarbital, 100 mg/kg, i.p., and perfused through the heart with 100 ml 0.1 M phosphate buffered saline (PBS), pH 7.3. Brains were removed and rapidly frozen in isopentane (−70 °C) cooled by acetone/dry ice bath. Parasagittal cryostat cut sections (10 or 20 μm) were thaw-mounted onto gelatin/chrome alum-coated slides and stored at −70 °C until used for in situ hybridization, immunohistochemistry or autoradiographic binding.

2.4.2. In situ hybridization

Antisense oligonucleotide probes complimentary to rat cDNA sequences [NR1, 5′-TCCTGCA GGTTCTTCCTCCACACGTTCACGGCTGCAAAAG CCAGCTGCATCTGCTTCCTA-3′; NR2A, 5′-CTCT GGAACTTCTTGTCACTGAGGCCAGTCACTTGGT-3′; NR2B, 5′-GAGTTGTTAAACACCAGACCCCA-GAGTAACCAAATTGCTTTGCCG-3′] were synthesized by Oligos Etc., Inc. (Willsonville, OR). Probes were 3′ end-labeled with [^{35}S]-dATP (12.5 mCi/ml, E.I. Dupont, Boston, MA) with terminal deoxytransferase (Boehringer Mannheim) as described previously (Tietz et al., 1999a). Prior to hybridization, sections were brought to room temperature under vacuum and fixed 5 min in 4% paraformaldehyde in 0.1 M PBS, pH 7.4.

2.4.2.1. Hybridization Using procedures identical to those previously used in our laboratory (Tietz et al., 1999a), sections were fixed, acetylated, dehydrated, defatted and stored under 95% EtOH at 20 °C until air-dried and prehybridized. Slides treated with RNAse 30 min at 37 °C prior to prehybridization were used as negative controls. For each [^{35}S]oligoprobe, one section per rat from both the experimental and control group was batch processed in parallel and handled identically. Sections were hybridized for 20 h at 43 °C in a humidified chamber with 70 μl/slide hybridization buffer containing 10 mM DTT, and 1×10^{-6} dpm [^{35}S]-labeled antisense oligoprobe/section under glass coverslips with parafilm bridges. Coverslips were removed in 1× SSC + DTT. Sections were washed 2 × [NR1 and NR2A: 1× SSC then 0.5× SSC 15 min at 55 °C; NR2B: 1× SSC at 60 °C × 15 min and one wash in 0.5× SSC at 22 °C], dehydrated, dried and apposed to Biomax MR film (Eastman Kodak Co., Rochester, NY).

2.4.3. Immunohistochemistry

FZP-treated and control rat brain sections were handled in parallel throughout all procedures, as described previously and validated (Chen et al., 1999; Van Sickle and Tietz, 2002a) with the following variations. Primary antibody (NR1: 1.5 μg/ml; NR2B: 1:1000) was applied to fixed and blocked (10% normal goat serum (v/v) plus 0.01% Triton X-100 (v/v) in PBS) tissue sections and incubated overnight at 4 °C. After 3 × 5 min PBS washes, FZP-treated and control sections were incubated with biotinylated anti-rabbit IgG F(ab′)$_2$ fragment (1:250 in PBS) for 1 h at room temperature. Sections were washed 3 × 5 min in PBS and incubated in avidin–biotin-peroxidase complex (1:100 v/v; Vector Laboratories, Burlingame, CA) for 1 h. Immunostaining was visualized in fresh 0.05% diaminobenzidine (DAB; Sigma) in PBS. Hydrogen peroxide (0.01%) was added immediately before the chromagen reaction was initiated. The DAB reaction was carried out for 1–2 min, the timing identical for FZP-treated and control sections. The reaction was stopped by 5 min PBS wash. Sections were dehydrated (75, 95, and 100% ethanol, 4 min each), cleared in xylene and coverslipped with Permount (Fisher, Pittsburgh, PA). Primary antibody was omitted from one section per experiment to serve as negative control.

2.4.4. Autoradiographic binding

Sections were pre-incubated at room temperature 2 × 5 min in buffer: 50 mM K_2HPO_4/NaH_2PO_4, 200 mM NaCl, 1 μM EDTA (pH 7.4), followed by 2 × 10 min in 50 mM Tris–HCl (pH 7.4) buffer containing 50 μM glutamate, 10 μM glycine, and 75 μM spermidine. Slides were dipped in 50 mM Tris–HCl then air dried. Sections were radiolabeled with the non-competitive NMDAR antagonist, [^{3}H]MK-801. Sections were incubated 1 h at room temperature in 50 mM Tris–HCl (pH 7.4) containing 50 μM glutamate, 10 μM glycine, 75 μM spermidine and 32 nM [^{3}H]MK-801 (Specific Activity, 21.7 Ci/mmol). Non-specific binding was determined in the presence of 10 μM unlabelled MK-801. Sections were washed 3 × 1 min in Tris–HCl buffer to remove unbound ligand then dipped in double distilled H_2O. Sections were rapidly dried, vapor-fixed with paraformaldehyde for 2 h at 80 °C under vacuum, exposed to [^{3}H]Hyperfilm (Amersham-Pharmacia, Arlington Heights, IL) for 2 weeks, and developed.

2.4.5. Image analysis

As described previously (Tietz et al., 1999a; Chen et al., 1999), images on film or slides were acquired under constant illumination by high resolution CCD camera (Sierra Scientific, Sunnyvale, CA) with the aid of NIH Image software (v. 1.62). Gray level measurements, which reflected mRNA expression, radioligand binding or subunit immunostaining density were made on digit-

ized images by delineating an area of interest using predetermined criteria to define the hippocampal subregions. For in situ hybridization and immunohistochemistry, background gray level was determined over the corpus callosum, a white matter area. Data were expressed as mean ± SEM of the raw gray level values. For receptor autoradiography, specific binding (total minus non-specific binding), expressed as pmol/mg protein, was estimated by linear regression analysis (r^2 = 0.99) of standard curves derived from gray level values over the same film exposed simultaneously to [^{3}H]thymidine brain paste standards. Non-specific binding gray levels were subtracted from gray levels representing total binding to give specific [^{3}H]MK-801 binding for each hippocampal subregion analyzed. Data were expressed as mean ± SEM of specific binding values (pmol/mg protein) for each brain region. All data were compared by repeated measures ANOVA. Post hoc comparisons were made using the method of Scheffé, with differences considered significant when $p \leq 0.05$.

3. Results

3.1. Electrophysiology

3.1.1. CA1 pyramidal neuron evoked NMDA-EPSCs after acute desalkyl-FZP treatment

Two days after a single dose of desalkyl-FZP (2.5 mg/kg p.o.) or control emulsion, whole-cell patch recordings were made in slices from acutely treated (141.6 ± 3.2 g) and control (138.5 ± 4.0 g) rats. Resting membrane potential immediately after whole-cell acquisition (CON: −63.7 ± 1.6 mV, $n = 6$; desalkyl-FZP: −66.0 ± 0.9 mV, $n = 7$; $p = 0.21$) was not significantly different between neurons from acute desalkyl-FZP and control emulsion-treated rats. In the presence of AMPA, $GABA_A$ and $GABA_B$ receptor antagonists, inward EPSCs were evoked in neurons voltage-clamped from −80 to +40 mV (Fig. 1A). These events were abolished by APV (50 μM), (data not shown), indicating that EPSCs represented NMDAR-mediated currents. There was no difference in the stimulation intensity required to elicit half-maximal currents (CON: 0.42 ± 0.05 mA; desalkyl-FZP: 0.35 ± 0.02 mA, $p = 0.16$), nor in CA1 neuron NMDA-EPSC amplitude at any holding potential from −80 to +40 mV (Fig. 1B).

3.1.2. CA1 pyramidal neuron evoked NMDA-EPSCs after 1-week FZP treatment

Whole-cell patch-clamp recordings were made from CA1 pyramidal neurons in hippocampal slices from 1-week FZP-treated (148.4 ± 2.8 mg/kg/week) and control rats (Fig. 1C). Resting membrane potential immediately after whole-cell acquisition (CON: −62.7 ± 0.9 mV, $n = 9$; FZP: −62.8 ± 1.0 mV, $n = 9$; $p = 0.93$) was not significantly different between FZP-treated and control neurons. Inward NMDAR-mediated EPSCs were evoked in neurons voltage-clamped from −80 to +40 mV (Fig. 1D). At holding potentials from −80 to −20 mV and at +40 mV, there was a significant decrease in the evoked NMDA-EPSC amplitude. The maximal significant difference was 52% reduction in evoked NMDA-EPSC amplitude at V_H = −20 mV. There was no difference in the stimulation intensity required to elicit half-maximal currents (CON: 0.29 ± 0.03 mA; FZP: 0.30 ± 0.04 mA, $p = 0.93$).

3.1.3. NMDA currents in acutely dissociated CA1 neurons after 1-week FZP treatment

Inward currents were elicited by NMDA at V_H = −30 mV and were abolished by omission of glycine. Glycine and strychnine alone had no effect. Peak current amplitude increased with increasing NMDA concentration (Fig. 2A, B). There was no significant ($p = 0.06$) difference in cell size, as estimated by cell capacitance, between the control (22.9 ± 1.8 pF, $n = 9$) and FZP-treated (18.3 ± 1.2 pF, $n = 8$) neurons sampled. Cell capacitance in cells isolated with protease XXIII for preliminary studies (data not shown) were similar (CON: 20.3 ± 1.3 pF, $n = 5$; FZP: 19.4 ± 1.2 pF, $n = 8$, $p = 0.60$). The maximal current elicited by NMDA was threefold greater, and the affinity 1.5–2 times less, in papain vs. protease XXIII-dissociated CA1 neurons (data not shown; F. Knoflach, personal communication) suggesting that unlike GABARs, NMDARs are substantially degraded by protease XXIII. As a function of NMDA concentration and maximal current amplitude, the duration of the response of neurons dissociated in papain was variable, lasting up to several minutes. As shown in Fig. 2C, increasing NMDA concentration resulted in a progressive increase in the peak amplitude of the response. Maximal current amplitude ranged from −254 to −2858 pA in papain-dissociated control cells and −98 to −1248 pA in FZP-treated cells. At higher concentrations, NMDA currents showed a biphasic response. This response was specific to NMDA application, and not likely due to the drug application system, since 30 μM GABA applied to the same neurons elicited an outward current with the expected activation rate and decay of the response (data not shown; Tietz et al., 1999b). Analysis of individual concentration–response curves indicated a significant ($p = 0.04$) 58% reduction in maximal NMDA-elicited currents in neurons dissociated from 1-week FZP-treated rats (FZP: I_{max} = −491.9 ± 128.4 pA, $n = 8$) in comparison to control CA1 neurons (CON: I_{max} = −1197.0 ± 253.8 pA, $n = 9$) without a significant change in EC_{50} (CON: 38.2 ± 4.4 μM, $n = 9$; FZP: 73.1 ± 22.3 μM, $n = 8$, $p = 0.50$). When normalized for cell capacitance (pA/pF), the average maximal currents were not signifi-

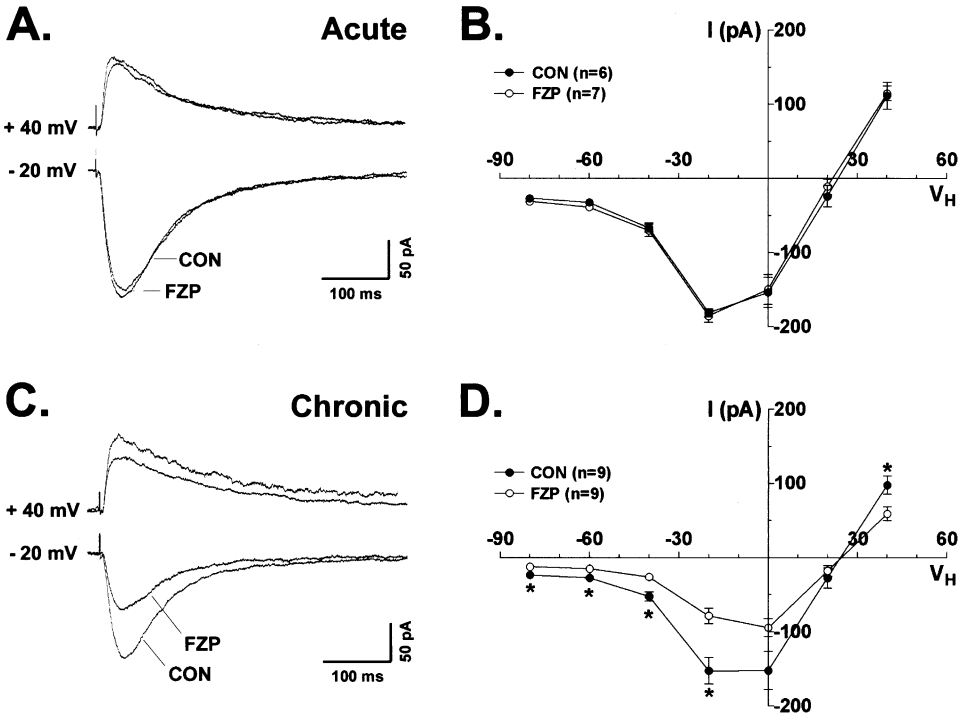

Fig. 1. NMDAR-mediated EPSCs evoked by Schaffer collateral stimulation of CA1 neurons in hippocampal slices from rats sacrificed 2 days after a single gavage of desalkylFZP or 1-week oral FZP treatment. A: Representative traces of evoked EPSCs generated at $V_H = -20$ and +40 mV in individual CA1 neurons from control and acute desalkylFZP-treated rats recorded in the presence of 1 mM $MgCl_2$, 10 μM glycine, 50 μM picrotoxin, 25 μM CGP-35348 and 10 μM DNQX. B: Averaged current–voltage (*I–V*) curves of peak evoked EPSC amplitude ($V_H = -80$ to +40 mV) generated in CA1 neurons from control (closed circles, $n = 6$ slices from 6 rats) and acute desalkylFZP-treated (open circles, $n = 7$ from 6 rats) rats. There was no significant shift in the *IV* curve across all holding potentials evaluated. C: Representative traces of NMDAR-mediated evoked EPSCs ($V_H = -20$ and +40 mV) recorded in individual CA1 neurons from a control rat and a 1-week FZP-treated rat. D: Averaged current–voltage (*I–V*) curves of peak evoked EPSC amplitude ($V_H = -80$ to +40 mV) generated in CA1 neurons from control (closed circles, $n = 9$ from 6 rats) and 1-week FZP-treated (open circles, $n = 9$ from 7 rats) rats. There was a significant decrease in NMDAR-mediated evoked EPSC amplitude, maximal (~50%) at −20 mV, indicated by a significant (∗) upward shift of the *IV* curve at holding potentials from −80 to −20 mV and downward shift at +40 mV. There were no significant differences in the stimulus intensity (0.3 mA) required to elicit half-maximal EPSCs between control and FZP-treated rats.

cantly different (CON: 54.1 ± 14.2 pA/pF; FZP: 27.9 ± 6.7 pA/pF, $p = 0.13$).

3.2. In situ hybridization

As described previously (Monyer et al., 1994), NMDA subunit mRNAs were most prominent in the hippocampal region in juvenile rats (Fig. 3A). There was a global effect of 1-week FZP treatment on NR1 subunit mRNA within the six hippocampal cell layers as indicated by a significant interaction of treatment × brain area (df = 1,5; $F = 0.9$, $p = 0.01$), however, post-hoc analysis by the method of Scheffé did not reveal selective modulation in any particular hippocampal region ($p = 0.18-0.96$). There were also no significant effects of 1-week FZP treatment on the levels of expression of the NR2A subunit in any hippocampal region (df = 1,5; $F = 0.81$, $p = 0.54$). The levels of expression of the NR2B subunit mRNA were significantly reduced (20%) in the CA1 cell layer (CON: 38.3 ± 2.5; FZP: 30.8 ± 2.3 density units, $p = 0.04$) as well as in the CA2 cell layer (−24%, CON: 37.0 ± 3.0; FZP: 28.1 ± 1.8 density units, $p = 0.02$; Fig. 3B). Though there was a trend towards a decreased (14%) NR2B mRNA expression in the DG cell region, it was not statistically significant ($p = 0.14$). No other cell layers showed an effect of chronic FZP treatment to reduce NR2B mRNA levels.

3.3. Quantitative immunohistochemistry

The relative NR1 and NR2B subunit antibody immunostaining patterns were similar to those described previously using light microscopic techniques (Petralia et al., 1994a,b), and in the absence of primary antibody, no immunostaining was observed. The intensity of NMDAR subunit immunostaining density over hippocampal somal and dendritic layers was compared in sections derived from FZP-treated and control rats to determine the relative amount of each antigen present (Fig. 4). On post hoc analysis, a significant effect of FZP treatment ($p < 0.05$) indicated a small (8.4%), significant

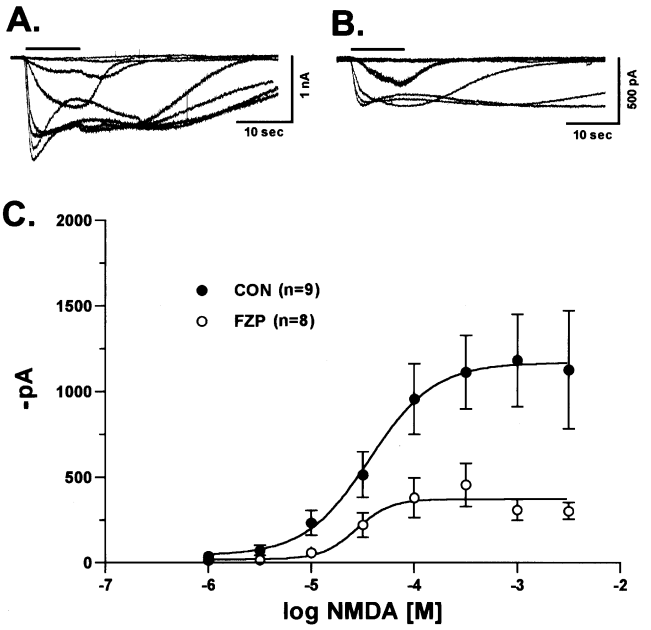

Fig. 2. NMDAR-mediated currents elicited in CA1 pyramidal neurons acutely dissociated from the hippocampus of rats sacrificed 2 days after 1-week oral FZP treatment. A: Representative, inward NMDA-mediated currents recorded ($V_H = -30$mV) in control papain-dissociated CA1 neurons in no-added Mg^{2+} buffer after U-tube application (10 s) of increasing concentrations of NMDA (1–3000 μM). B: Representative NMDA-mediated currents in a CA1 neuron dissociated from a 1-week FZP-treated rat hippocampus. C: NMDA-induced concentration-response (1–3000 μM). There was no significant shift ($p = 0.50$) in the EC_{50} in individual control ($n = 9$ from 5 rats) and 1-week FZP-treated ($n = 8$ from 5 rats) dissociated neurons. The maximal current elicited by NMDA application was significantly decreased ($p = 0.04$) in individual CA1 neurons from FZP-treated rats in comparison to controls. The fit of the pooled data from dissociated neurons from control ($EC_{50} = 37.1$ μM; $I_{max} = -1170 \pm 24.5$ pA) and 1-week FZP-treated rats ($EC_{50} = 27.5$ μM; $I_{max} = -373.4 \pm 35.2$ pA) is illustrated in C.

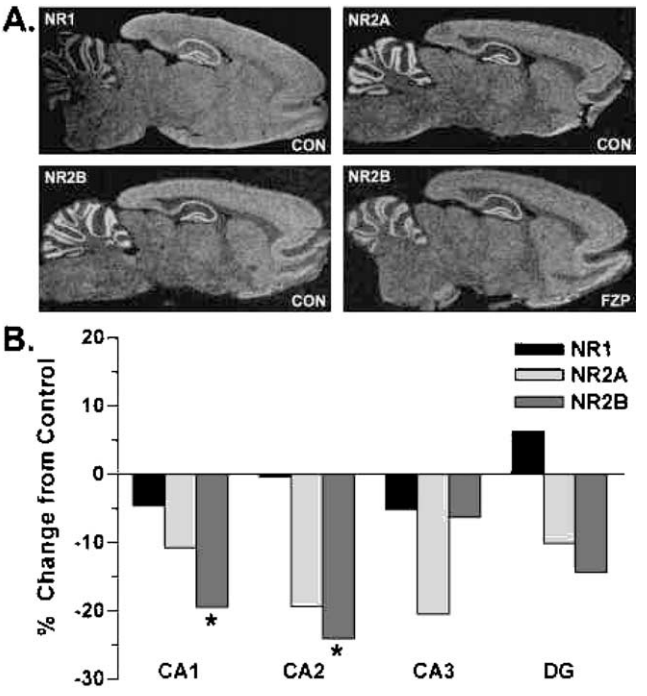

Fig. 3. Expression of NMDAR subunit mRNA levels in selected subregions of the hippocampus in control rats and rats sacrificed 2 days after 1-week oral FZP treatment. Brain sections (10 μm) from control and FZP-treated rats were hybridized with antisense [^{35}S]oligoprobes to the NR1, N2A and NR2B subunits of the NMDA receptor. Regional variations in mRNA expression were examined using computer-assisted image analysis. A, Top: Images representative of NR1 and NR2A mRNA levels in control (CON) rats. A, Bottom: Images representative of NR2B mRNA levels in control (CON) and 1-week FZP-treated (FZP) rats. B: Percent change from control of the relative density over hippocampal cell layers hybridized with the NR1 (black bars), NR2A (light gray bars) and NR2B (dark gray bars) oligoprobes. There were significant decreases in the levels of expression of the NR2B, but not NR1 or NR2A, mRNA in CA1 and CA2 neurons from 1-week FZP-treated rats. Asterisks denote significant differences $p \leq 0.05$ in mean relative gray level values between brain sections from control and FZP-treated rats ($n = 8$ rats per group, one section per rat).

decrease in NR1 subunit immunostaining (Fig. 4A) only in the stratum pyramidale (SP) of the CA1 region (CON: 32.1 ± 0.7; FZP: 29.4 ± 0.9 density units, $p = 0.02$; $n = 8$ rats per group, one section per rat). There were no other changes in NR1 subunit immunostaining in any hippocampal region measured. Consistent with the decreased levels of NR2B mRNA (Fig. 3B), NR2B subunit immunostaining density was significantly reduced (~18%) in the basilar dendritic (stratum oriens (SO), CON: 18.6 ± 0.9; FZP: 15.3 ± 0.9 density units, $p = 0.02$) and somal (SP, CON: 25.5 ± 1.9; FZP: 20.7 ± 1.4 density units, $p = 0.04$) regions of area CA1. Likewise, the SO (CON: 15.5 ± 1.2; FZP: 11.5 ± 0.9 density units, $p = 0.01$) and SP (CON: 24.1 ± 1.9; FZP: 17.9 ± 1.2 density units, $p = 0.01$) regions of area CA2 also showed somewhat greater reduction in NR2B immunostaining density. Significant changes were not detected in any other hippocampal region in FZP-treated rats (Fig. 4B). An NR2A subunit antibody (Affinity Bioreagents) proved unsatisfactory for immunohistochemical staining.

3.4. [^{3}H]MK-801 Autoradiography

The total number of hippocampal NMDARs was investigated by quantitative receptor autoradiography using a saturating concentration (32 nM) of [^{3}H]MK-801. The density of the film images over radiolabeled hippocampal regions of 1-week FZP treated ($n = 7$) and control ($n = 6$) rat brain sections was compared to the film density over [^{3}H]thymidine brain paste-standards to estimate specific [^{3}H]MK-801 binding (pmol/mg protein) (Fig. 5A). Non-specific binding values were ~15% of total binding. Specific [^{3}H]MK-801 binding was greatest in the CA1 dendritic regions (SO, CON: 1.57 ± 0.15; FZP: 1.62 ± 0.08 pmol/mg protein; SR, CON: 1.98 ± 0.25; FZP: 2.08 ± 0.11 pmol/mg protein)

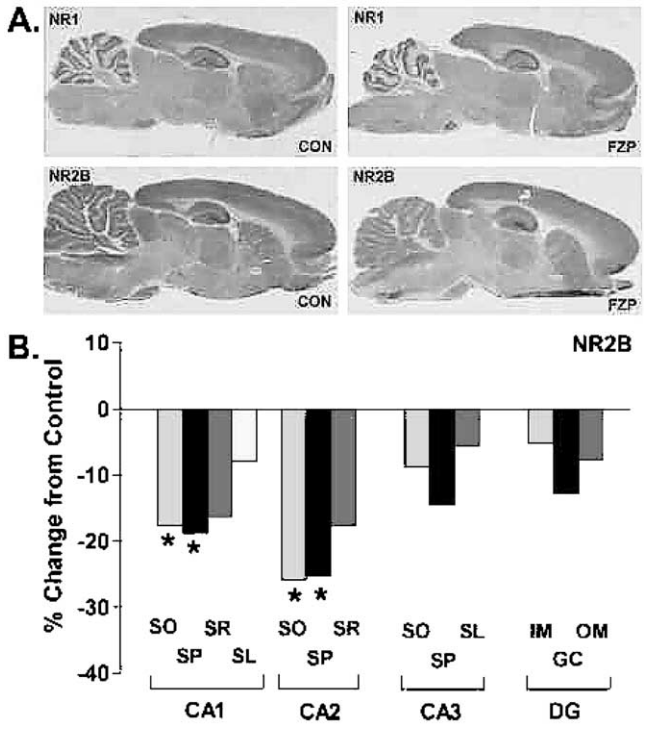

Fig. 4. Levels of NMDAR NR2B subunit immunostaining in selected subregions of the hippocampus in control rats and rats sacrificed 2 days after 1-week oral FZP treatment. Brain sections (20 μm) from control and FZP-treated rats were immunostained with an NR2B subunit specific antibody. Regional variations in immunohistochemical staining were examined using computer-assisted image analysis. A: Relative distribution of NR2B immunostaining in representative sections from control (CON) and FZP-treated (FZP) rats. B: Quantitation of NR2B immunostaining density in hippocampal subregions from FZP-treated rats expressed as percent change from control. A significant decrease in mean relative gray level was detected in the SO and SP of areas CA1 and CA2. No significant differences in NR2B immunostaining density were detected between FZP-treated and control rats in any other hippocampal region. Asterisks denote significant $p \leq 0.05$ differences in mean (±SEM) relative gray level values between brain sections from control and FZP-treated rats ($n = 8$ rats per group, one section per group). CA1–CA3: SO, stratum oriens; SP, stratum pyramidale; SR, stratum radiatum; SL, stratum lancunosum-moleculare (CA1) or stratum lucidum (CA3); dentate gyrus (DG): IM, inner molecular; OM, outer molecular; GC, granule cell layers.

as well as the CA2 dendritic regions (SO, CON: 1.04 ± 0.11; FZP: 0.93 ± .09 pmol/mg protein; SR, CON: 1.48 ± 0.22; FZP: 1.42 ± 0.11 pmol/mg protein). Binding was also prominent in the dentate gyrus molecular layer (CON: 1.38 ± 0.17; FZP: 1.47 ± 0.12 pmol/mg protein) but was lower in hippocampal cell layers (range: 0.34–1.12 pmol/mg protein). Comparisons of specific [^{3}H]MK-801 binding density in hippocampal regions indicated no significant (df = 1,12; $F = 0.069$, $p = 0.80$) changes in the total number of hippocampal NMDAR binding sites (Fig. 5B).

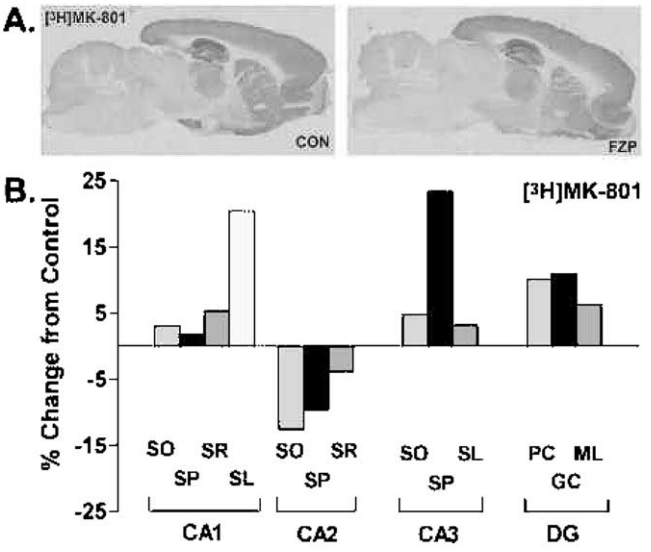

Fig. 5. NMDAR antagonist, [^{3}H]MK-801, binding in selective hippocampal subregions of the hippocampus in rats sacrificed 2 days after 1-week oral FZP treatment. Parasagittal brain sections (20 μm) were incubated with a saturating concentration (32 nM) of [^{3}H]MK-801 and exposed to [^{3}H]-sensitive film for 2 weeks with [^{3}H]thymidine brain paste standards A: Representative images of total [^{3}H]MK-801 binding in whole brain from control (CON) and FZP-treated (FZP) rats. Nonspecific binding, in the presence of 10 μM MK-801, was subtracted to estimate specific binding. B: Quantitation of specific [^{3}H]MK-801 binding in hippocampal subregions from FZP-treated rats expressed as percent change from control specific binding. Specific binding was greatest in the dendritic regions of the CA1 and CA2 (SO and SP) regions, as well as the dentate gyrus (MOL) (range: 1.0–2.0 pmol/mg protein). Specific binding in cell layers was less dense (range: 0.3–1.0 pmol/mg protein), thus small changes reflect a larger percent change. No significant decreases in [^{3}H]MK-801 binding were found in any hippocampal subregion analyzed. The apparent difference in [^{3}H]MK-801 binding in substantia nigra in the control and FZP-treated sections illustrated may merit further investigation, but was beyond the scope of the present paper. CA1–CA3: SO, stratum oriens; SP, stratum pyramidale; SR, stratum radiatum; SL, stratum lancunosum-moleculare (CA1) or stratum lucidum (CA3); dentate gyrus (DG): PC, polymorph cells (CA4); ML, molecular layer; GC, granule cell layer.

4. Discussion

The findings of this study support the hypothesis that an altered balance of excitation and inhibition in CA1 pyramidal neurons during chronic in vivo potentiation of GABARs by BZs, results in regulation of NMDAR function and expression. In the present study, a significant reduction in postsynaptic NMDAR-mediated currents was detected in CA1 pyramidal neurons in in vitro hippocampal slices, as well as in acutely dissociated CA1 neurons, 2 days after ending a chronic BZ treatment which reliably and selectively decreases synaptic inhibition (Zeng et al., 1995; Poisbeau et al., 1997; Zeng and Tietz, 1999) and increases synaptic excitation (Van Sickle and Tietz, 2002a) in this same neuron population. Additionally, the reduced NMDAR function was correlated with specific decreases in the expression of the NR2B subunit mRNA and protein. Importantly, the

reduction in NMDAR function was not present following acute BZ administration. Given the central role for NMDARs in mediating activity-dependent synaptic modification in the CA1 region, these changes in NMDAR function and expression may reflect the adaptive processes within the hippocampus which occur with chronic BZ administration and contribute to BZ tolerance, and perhaps dependence.

4.1. Electrophysiology

Following chronic BZ exposure, alteration in synaptic excitatory and inhibitory receptor function may result in sufficient membrane depolarization to permit enhanced activation of synaptic NMDARs. During excitatory synaptic transmission, AMPAR activation is a well-established source for the membrane depolarization required for gating of NMDARs. Since AMPARs and NMDARs are co-localized at CA1 dendritic synapses (He et al., 1998), enhanced AMPAR-mediated function in CA1 pyramidal neurons from 1-week FZP-treated rats may initially contribute to an enhancement of NMDAR activation. Indeed, preliminary studies demonstrate significantly increased AMPAR-mediated function 1 day after 1-week FZP treatment (Van Sickle and Tietz, 2002b). The presence of a GABAR-mediated depolarizing potential, in CA1 neurons from FZP-treated rats, provides another possible mechanism for relief of the Mg^{2+} block of NMDARs. The GABAR-mediated depolarizing potential can be elicited in CA1 neurons following experimental manipulations (Alger and Nicoll, 1982; Staley et al., 1995), however, physiological patterns of stimulation can also result in GABAR-mediated depolarization as a result of intracellular Cl^- accumulation (Bracci et al., 2001). Moreover, the depolarization permits a disinhibition of the local network in the CA1 region and facilitates excitatory neurotransmission (Bracci et al., 2001). In addition, Staley et al. (1995) reported that NMDAR-mediated conductance was increased 10-fold by the GABAR-mediated depolarizing potential, suggesting that it can provide activity-dependent modulation of the Mg^{2+} block of NMDARs. Given the appearance of depolarizing potentials in FZP-treated rats without high-frequency stimulation or other experimental manipulations (Zeng et al., 1995), the possibility that NMDAR activation in CA1 pyramidal neurons is transiently enhanced and subsequently downregulated in association with chronic BZ administration appears quite plausible.

Increased activation of NMDARs due to increased AMPAR activation (Van Sickle and Tietz, 2002a) and/or the GABAR depolarizing response (Zeng et al., 1995) may be predicted to induce downregulation of NMDAR function in CA1 neurons. Indeed, evoked-NMDAR EPSCs are reduced to a maximum of 52% ($V_H = -20$mV) in CA1 neurons recorded in hippocampal slices (Fig. 1D) from 1-week FZP-treated rats. Resting membrane potential and the stimulus intensity required to elicit NMDAR EPSCs are not different between control and 1-week FZP-treated rats suggesting that reduced NMDAR function does not result from alteration in the intrinsic neuronal membrane properties of CA1 neurons. Moreover, absence of a change in the characteristic 'J-shape' or reversal potential of the *I–V* curve of evoked NMDAR EPSCs suggests that Mg^{2+} sensitivity of NMDARs is not altered in CA1 neurons following 1-week FZP treatment. It would have been helpful to record NMDAR-mediated mEPSCs in CA1 neurons to determine the kinetic properties of postsynaptic NMDARs in the hippocampal slice preparation, unfortunately, NMDAR mEPSCs are only present in immature neurons. Efforts were made to observe them under conditions that enhance NMDAR currents (low Mg^{2+}, elevated pH), however these proved unsuccessful. The lack of effect of acute desalkyl-FZP treatment on the evoked NMDAR-EPSC amplitude indicates that the reduction in NMDAR-mediated function is specific to chronic BZ administration. Moreover, it suggests a mechanism which requires persistent modulation of inhibitory activity and is dependent upon changes that occur with long-term administration of BZs. Multiple mechanisms, including changes in NMDAR number, conductance, kinetic properties or subunit composition could account for decreased postsynaptic NMDAR function in CA1 pyramidal neurons.

To examine postsynaptic NMDAR function in the absence of presynaptic influences, NMDA-induced currents were recorded in acutely dissociated CA1 neurons from control and FZP-treated rats. The 58% reduction in maximal current (I_{max}) in acutely dissociated neurons, after chronic FZP administration (Fig. 2C) is consistent with the decreased NMDAR function in intact CA1 neurons in vitro. In the absence of a change in the apparent affinity (EC_{50}) of NMDA, the findings in both slices and dissociated neurons suggest a reduction in the number of postsynaptic NMDARs or in NMDAR conductance in CA1 neurons. This reduction could not be accounted for by decreased cell size, since cell capacitance measurements were not different between groups. Maximal currents normalized for cell capacitance were not statistically different between groups, but showed the same trend, with current densities about 48% smaller in neurons from FZP-treated rats. However, measures of cell area using cell capacitance may result in a poor estimate of current density (Ebihara et al., 1992), since acutely dissociated pyramidal neurons maintain their gross morphological characteristics, i.e. large cell body and extended dendrites, and capacitance measures are only accurate for small spherical cells.

Using a drug application method without rapid displacement of applied drug, no definitive conclusion can be drawn regarding the kinetics of the NMDA-mediated

off response. Ultra-rapid drug application techniques are necessary to detect the offset kinetics characteristic of native and recombinant NR2A and NR2B-containing NMDARs (Monyer et al., 1994; Kew et al., 1998). Thus, such a more refined approach will be helpful in determining whether a change in the relative proportion of these receptor isoforms contributed to decreased NMDAR-mediated responses after chronic FZP.

4.2. In situ hybridization, immunohistochemistry and autoradiography

The subunit composition of NMDARs is an important determinant of their functional properties. Studies of recombinant NMDARs have demonstrated the importance of the NR2 subunit in determining receptor properties such as Mg^{2+} sensitivity, offset kinetics of glutamate-induced currents and affinity for different modulators and antagonists (Monyer et al., 1994; Vicini et al., 1998). Co-immunoprecipitation studies of cortical membranes suggests that native adult forebrain NMDARs are composed of NR1/NR2A, NR1/NR2B and NR1/NR2A/NR2B complexes (Sheng et al., 1994; Blahos and Wenthold, 1996; Luo et al., 1997) with a significant proportion (up to ~50%) of complexes containing NR1/NR2A/NR2B (Luo et al., 1997). Moreover, three pharmacologically identifiable populations of NMDARs are found in single adult parietal cortex neurons (Kew et al., 1998), corresponding to the functional and pharmacological properties of recombinant NMDARs in cells transfected with different ratios of NR1, NR2A and NR2B subunit cDNAs (Vicini et al., 1998). In hippocampus, NR1, NR2A and NR2B subunit mRNAs (Monyer et al., 1994) and proteins (Petralia et al., 1994a, 1994b) are abundantly expressed suggesting that NMDARs in hippocampal neurons likely also consist of di- and triheteromeric complexes of NR1 with NR2 subunits.

It is interesting that NR2B subunit mRNA and protein were downregulated only in specific hippocampal subregions following chronic FZP treatment. This would suggest reduced incorporation of NR2B subunits into triheteromeric CA1 (and CA2) NMDARs or a decrease in the population of NR1–NR2B receptor complexes. Such a change in NMDAR composition or number would be predicted to result in decreased synaptic NMDAR-mediated currents, which is indeed the case in this study. In addition, since NR1 subunits are required for functional NMDARs, the small (8%), but significant, decrease in NR1 subunit protein in the CA1 pyramidal cell layer of 1-week FZP-treated rats also suggests a reduction in NMDAR number. The possibility of decreased NMDAR number was examined using a saturating concentration of the non-competitive NMDAR antagonist [^{3}H]MK801. There was no change in specific binding in the CA1 (or CA2) region suggesting that the total number of NMDARs was unchanged, however this does not preclude a selective decrease in NR2B-containing NMDARs. Preliminary autoradiographic binding studies with [^{3}H]ifenprodil, which is selective for NR2B-containing NMDARs (Nicolas and Carter, 1994), were inconclusive (data not shown) but may provide a useful tool for detecting decreased NR1–NR2B-containing NMDARs after chronic BZ treatment. As excitatory synapses have been localized to dendritic regions of the hippocampus (Papp et al., 2001), reductions in NR1 and NR2B subunit proteins detected in CA1 and CA2 pyramidal cell body layers may represent changes in unassembled NR subunits or in extrasynaptic NMDARs localized to the cell body. Extrasynaptic NMDARs have been shown to play a functional role in CA1 pyramidal neurons (Garaschuk et al., 1996), therefore, further studies are necessary to determine if extrasynaptic NMDARs were also regulated by chronic BZ treatment.

4.3. NMDARs in BZ tolerance/dependence

NMDARs are thought to play a role in the neuroadaptive processes associated with tolerance and dependence to several drugs of abuse, including CNS depressants (Trujillo and Akil, 1995). The ability of NMDAR antagonists to block development of tolerance and expression of dependence signs after long-term treatment with diazepam suggests that NMDAR-dependent mechanisms are involved (Steppuhn and Turski, 1993). Furthermore, chronic exposure to barbiturates, which also facilitate GABAR-mediated inhibition, results in selective decreases in NR2B subunit mRNA in the CA1 region of hippocampus without changes in NR1 or NR2A mRNAs (Jang et al., 1998). These changes in NMDAR subunit expression are similar to the findings presented in this study and suggest a common role for NMDARs in tolerance and dependence to CNS depressants acting through GABARs. The mechanism responsible for the specific reduction in NR2B subunit mRNA and protein following chronic BZ exposure remains to be determined, however, activity-dependent increases in intracellular Ca^{2+} can lead to selective downregulation of NR2B expression (Vallano et al., 1996). Interestingly, expression of NR2B subunits in cerebellar granule neurons, in vitro, is selectively increased by inhibition of the Ca^{2+}/calmodulin-dependent protein kinases (CaM kinases) (Corsi et al., 1998). Since NMDARs are highly permeable to Ca^{2+}, one can hypothesize that NMDAR-mediated Ca^{2+} flux activates CaM kinases to regulate expression of NR2B subunit protein. Following chronic FZP treatment, the transient activation of NMDARs by increased AMPAR function and the GABAR-mediated depolarizing response, as discussed above, could increase Ca^{2+} flux into CA1 neurons, activate CaM kinases and result in the decreased NR2B mRNA and protein expression observed in this study. Further studies

are needed to evaluate the mechanisms involved in NMDAR regulation following chronic BZ exposure and the role this regulation plays in the adaptive processes involved in BZ tolerance and dependence.

4.4. Conclusion

The current study establishes decreased NMDAR-mediated neurotransmission in CA1 pyramidal neurons in in vitro hippocampal slices as well as in dissociated CA1 pyramidal neurons following chronic BZ treatment. Moreover, reduced NMDAR function is accompanied by reductions in NMDAR subunit NR2B mRNA and protein in the hippocampal CA1 region. The downregulation of postsynaptic NMDAR function and NR2B subunit expression may be a compensatory response to increased NMDAR activation resulting from the altered excitatory–inhibitory balance in CA1 neurons after chronic BZ exposure. These data suggest a dynamic balance between excitation and inhibition in the CA1 region following chronic BZ exposure and support a role for NMDAR-dependent mechanisms in the development and/or expression of BZ anticonvulsant tolerance and dependence.

Acknowledgements

We would like to thank Eugene Orlowski and Anne Lyons for technical assistance. This work was supported by National Institutes of Health grants R01-DA0475 (to E.I.T.), F30-DA0604 (to B.J.V.) and a predoctoral fellowship (to B.J.V.) from the Medical College of Ohio

References

Alger, B.E., Nicoll, R.A., 1982. Feed-forward dendritic inhibition in rat hippocampal pyramidal cells studied in vitro. Journal of Physiology 328, 105–123.

Blahos, J. II, Wenthold, R.J., 1996. Relationship between *N*-methyl-D-aspartate receptor NR1 splice variants and NR2 subunits. Journal of Biological Chemistry 271, 15669–15674.

Bracci, E., Vreugdenhil, M., Hack, S.P., Jefferys, J.G.R., 2001. Dynamic modulation of excitation and inhibition during stimulation at gamma and beta frequencies in the CA1 hippocampal region. Journal of Neurophysiology 85, 2412–2422.

Chen, S., Huang, X., Zeng, X.J., Sieghart, W., Tietz, E.I., 1999. Benzodiazepine-mediated regulation of α1, α2, β1-3 and γ2 $GABA_A$ receptor subunit proteins in the rat brain hippocampus and cortex. Neuroscience 93, 33–44.

Corsi, L., Li, J.H., Krueger, K.E., Wang, Y.H., Wolfe, B.B., Vicini, S., 1998. Up-regulation of NR2B subunit of NMDA receptors in cerebellar granule neurons by Ca^{2+}/calmodulin kinase inhibitor KN93. Journal of Neurochemistry 70, 1898–1906.

Ebihara, S., Takishima, T., Shirasaki, T., Akaike, N., 1992. Regional variation of excitatory and inhibitory amino acid-induced responses in rat dissociated CNS neurons. Neuroscience Research 14, 61–71.

Garaschuk, O., Schneggenburger, R., Schirra, C., Tempia, F., Konnerth, A., 1996. Fractional Ca^{2+} currents through somatic and dendritic glutamate receptor channels of rat hippocampal CA1 pyramidal neurons. Journal of Physiology 491, 757–772.

Greenfield, L.J., Macdonald, R.L., 1996. Whole cell and single channel α1β1γ2S $GABA_A$ receptor currents elicited by a multipuffer drug application device. Pflüger's Archiv European Journal of Physiology 432, 1080–1090.

He, Y., Janssen, W.G.M., Morrison, J.H., 1998. Synaptic coexistence of AMPA and NMDA receptors in the rat hippocampus: a postembedding immunogold study. Journal of Neuroscience Research 54, 444–449.

Hutchinson, M.A., Smith, P.F., Darlington, C.L., 1996. The behavioural and neuronal effects of the chronic administration of benzodiazepine anxiolytic and hypnotic drugs. Progress in Neurobiology 49, 73–97.

Jang, C.G., Oh, S., Ho, I.K., 1998. Changes in NMDAR2 subunit mRNA levels during pentobarbital tolerance/withdrawal in the rat brain: an in situ hybridization study. Neurochemical Research 23, 1371–1377.

Kew, J.N.C., Richards, J.G., Mutel, V., Kemp, J.A., 1998. Developmental changes in NMDA receptor glycine affinity and ifenprodil sensitivity reveal three distinct populations of NMDA receptors in individual rat cortical neurons. Journal of Neuroscience 18, 1935–1943.

Luo, J., Wang, Y., Yasuda, R.P., Dunah, A.W., Wolfe, B.B., 1997. The majority of N-methyl-D-asparate receptor complexes in adult rat cerebral cortex contain at least three different subunits (NR1/NR2A/NR2B). Molecular Pharmacology 51, 79–86.

Macdonald, R.L., Olsen, R.W., 1994. $GABA_A$ receptor channels. Annual Review of Neuroscience 17, 569–602.

Monyer, H., Burnashev, N., Laurie, D.J., Sakmann, B., Seeburg, P.H., 1994. Developmental and regional expression in the rat brain and functional properties of four NMDA receptors. Neuron 12, 529–540.

Nicolas, C., Carter, C., 1994. Autoradiographic distribution and characteristics of high- and low-affinity polyamine-sensitive [^{3}H]Ifenprodil sites in the rat brain: possible relationship to NMDAR2B receptors and calmodulin. Journal of Neurochemistry 63, 2248–2258.

Papp, E., Leinekugel, X., Henze, D.A., Lee, J., Buzsaki, G., 2001. The apical shaft of CA1 pyramidal cells is under GABAergic interneuronal control. Neuroscience 102, 715–721.

Petralia, R.S., Yokotani, N., Wenthold, R.J., 1994a. Light and electron microscope distribution of the NMDA receptor subunit NMDAR1 in the rat nervous system using a selective anti-peptide antibody. Journal of Neuroscience 14, 667–696.

Petralia, R.S., Wang, Y.-X., Wenthold, R.J., 1994b. The NMDA receptor subunits NR2A and NR2B show histological and ultrastructural localization patterns similar to those of NR1. Journal of Neuroscience 14, 6102–6120.

Poisbeau, P., Williams, S., Mody, I., 1997. Silent $GABA_A$ synapses during flurazepam withdrawal are region specific in the hippocampal formation. Journal of Neuroscience 17, 3467–3475.

Rosenberg, H.C., 1995. Differential expression of benzodiazepine anticonvulsant cross-tolerance according to time following flurazepam or diazepam treatment. Pharmacology, Biochemistry and Behavior 51, 363–368.

Sheng, M., Cummings, J., Roldan, L.A., Jan, Y.N., Jan, L.Y., 1994. Changing subunit composition of heteromeric NMDA receptors during development of rat cortex. Nature 368, 144–147.

Staley, K.J., Soldo, B.L., Proctor, W.R., 1995. Ionic mechanisms of neuronal excitation by inhibitory $GABA_A$ receptors. Science 269, 977–981.

Steppuhn, K.G., Turski, L., 1993. Diazepam dependence prevented by glutamate antagonists. Proceedings of the National Academy of Science 90, 6889–6893.

Tietz, E.I., Huang, X., Chen, S., Ferencak, W.J. III, 1999a. Temporal

and regional regulation of α1, β2 and β3, but not α2, α4, α5, α6, β1 or γ2 $GABA_A$ receptor subunit mRNAs following one week oral flurazepam administration. Neuroscience 91, 327–341.

Tietz, E.I., Kapur, J., Macdonald, R.L., 1999b. Functional $GABA_A$ receptor heterogeneity of acutely dissociated hippocampal CA1 pyramidal cells. Journal of Neurophysiology 81, 1575–1586.

Trujillo, K.A., Akil, H., 1995. Excitatory amino acids and drugs of abuse: a role for *N*-methyl-D-aspartate receptors in drug tolerance, sensitization and physical dependence. Drug and Alcohol Dependence 38, 139–154.

Vallano, M.L., Lambolez, B., Audinat, E., Rossier, J., 1996. Neuronal activity differentially regulates NMDA receptor subunit expression in cerebellar granule cells. Journal of Neuroscience 16, 631–639.

Van Sickle, B.J., Tietz, E.I., 2002a. Selective enhancement of AMPA receptor-mediated function in hippocampal CA1 neurons from chronic flurazepam-treated rats. Neuropharmacology 43, 11–27.

Van Sickle, B.J., Tietz, E.I., 2002b. Transient benzodiazepine-induced plasticity of CA1 excitatory and inhibitory synapses relates to benzodiazepine dependence. Society for Neuroscience Abstracts (available on CD).

Vicini, S., Wang, J.F., Li, J.H., Zhu, W.J., Wang, Y.H., Luo, J.H., Wolfe, B.B., Grayson, D.R., 1998. Functional and pharmacological differences between recombinant N-methyl-D-aspartate receptors. Journal of Neurophysiology 79, 555–566.

Xie, X.H., Tietz, E.I., 1992. Reduction in potency of selective γ-aminobutyric $acid_A$ agonists and diazepam in CA1 region of in vitro hippocampal slices from chronic flurazepam-treated rats. Journal of Pharmacology and Experimental Therapeutics 262, 204–211.

Zeng, X., Xie, X.H., Tietz, E.I., 1995. Reduction of GABA-mediated IPSPs in hippocampal CA1 pyramidal neurons following oral flurazepam administration. Neuroscience 66, 87–99.

Zeng, X., Tietz, E.I., 1999. Benzodiazepine tolerance at GABAergic synapses on hippocampal CA1 pyramidal cells. Synapse 31, 263–277.